Chalcogenide Letters Vol. 11, No. 5, May 2014, p. 199 - 207

SYNTHESIS AND TRIBOLOGICAL PROPERTIES OF Ti-DOPED $NbSe_2$ NANOPARTICLES

Q. SHI[a,b], H. TANG[c], H. ZHU [a,b], G. TANG[a], K. ZHANG[c], H. ZHANG[c], C. LI[a,c*]

[a]*School of Mechanical Engineering, Jiangsu University, Key Laboratory of Tribology of Jiangsu Province, Zhenjiang 212013, Jiangsu Province, China*

[b]*School of Mechanical Engineering, Zhenjiang Vocational Technical College, Zhenjiang 212016, Jiangsu Province, China*

[c]*School of Materials Science and Engineering, Jiangsu University, Zhenjiang 212013, Jiangsu Province, China*

Ti-doped $NbSe_2$ nanobelts along with nanoplates have been successfully fabricated via a facile solid-state thermal reaction using micro-sized Ti, Nb and Se elements as raw materials. The morphology and structure of the as-prepared products were investigated by X-ray diffractometer (XRD)、scanning electron microscopy (SEM). The morphology of Ti-doped $NbSe_2$ samples obtained at the reaction temperature of 700°C are composed of thin and long belts-like structures which have a width in the range of 50nm–600nm and the length about a few microns, while at the reaction temperature of 800°C the as-preapred Nb1-xTixSe2 products are mainly composed of a large amount of nanoplates with diameters of about 500 nm−3 μm and the thickness of about 30 nm−500 nm. It was also found that the sizes of the sample evidently reduced while the contents of dopant increased within a certain limit (1at.%−9at.%). Moreover, the tribological properties of the Ti-doped $NbSe_2$ nanobelts/nanoplates were investigated. Experimental results indicated that the addition of both $Nb_{1-x}Ti_xSe_2$ nanobelts/nanoplates improve the tribological properties of paraffin base oil, furthermore the friction coefficient of the base oil containing Ti-doped $NbSe_2$ nanoplates was lower and more stable than those of pure $NbSe_2$ nanoplates and Ti-doped $Nbse_2$ nanobelts.

(Received March 9, 2014; Accepted April 30, 2014)

Keyword: Tribological properties, Solid-state reaction, Nanobelts and nanoplates, Ti-doped $NbSe_2$

1. Introduction

Over the past few decades, transition metal dichalcogenides have attracted much attention owing to their unique properties such as superconducting, thermoelectric, lubricative and magnetic behaviors. Transition metal dichalcogenides such as $NbSe_2$, NbS_2,$TaSe_2$, MoS_2, $MoSe_2$ and $TiSe_2$, have hexagonal structures which atoms within a layer are bound covalently and separate layers are held together mainly through weak Van der Waals interactions[1-5]. Molybdenum disulfide (MoS_2) with special layered close-packed hexagonal crystal structure is one of typical layered compounds, which is particularly important for solid lubrication or as an additive for lubricating oils and greases and has enjoyed the reputation of “the king of lubrication” for a long time. $NbSe_2$ and

*Corresponding author: lichangshengujs@yahoo.com

$TiSe_2$ which with the similar crystalline structure and tribological properties of MoS_2, but the electrical resistivity of $NbSe_2$ is about only $3.5\times10^{-4}\,\Omega \bullet$ cm that six amount levels less than that of MoS_2. Although $NbSe_2$ and $TiSe_2$ have many advantages, however, to the author's knowledge, reports about the friction and wear behavior of them are very rare.

Doping is one of effective ways to improve material performance in many research fields such as photocatalytic materials, lithium-ion battery materials, information materials, magnetic materials, etc. Doping nanocrystals provides another fundamental approach to modify the properties of nanocrystals by means of tailoring the crystal's compositions [13-16]. It is confirmed that doping can bring about changes in c-axis lattice constant and electronic structure. For example, Hu et al. [19-20] researched the electrical and optical properties of niobium and rhenium doped $MoSe_2$. Zhang et al. [11-12] researched the tribological properties of tungsten doped $MoSe_2$ and niobium doped $MoSe_2$. Recently, researchers had done a lot of research on doping modification of $NbSe_2$, for instance of doping comparatively cheap Co, Mn, Cu into $NbSe_2$ [6–10], but they mainly focus on the superconductivity, CDW, photoemission or performance of magnetization. It has been reported that alloying between $NbSe_2$ and $TiSe_2$ causes quite interesting physical properties which are absent in both end materials. However, until recently, very little research has been performed to understand the tribological properties of titanium doped $NbSe_2$.

In this paper, Ti-doped $NbSe_2$ nanobelts/nanoplates have been successfully fabricated by a facile solid-state reaction. The products were characterised by an X-ray diffractometer (XRD) and scanning electron microscopy (SEM). The SEM images showed the introduction of Ti dopant leaded to an obvious size reduction of nanoparticles. Moreover, the tribological properties of $Nb_{1-x}Ti_xSe_2$ nanobelts/nanoplates as additives in paraffin base oil were also investigated and Ti-doped $NbSe_2$ nanoparticles exhibited a better friction and wear property than $NbSe_2$ as additives in paraffin base oil.

2. Experiment

2.1 Synthesis of $NbSe_2$ and Ti-doped $NbSe_2$ nanobelts and nanoplates

In this experiment, elemental selenium (99.9%, 300 mesh), titanium(99.9%, 300 mesh) and niobium(99.8%, 200 mesh) powders were purchased from Shanghai Chemical Reagent Co. Ltd. (Shanghai, China). All chemical reagents were of analytic purity and used directly without further purification.

Table 1 Summary of the Samples Doped with Different Amounts of Ti powders.

Sample	Ti-containing	Ti:Nb:Se/mole ratio	Sample	Ti-containing	Ti:Nb:Se/mole ratio
Sa1	0	0:100:205	Sa4	9%	9:91:205
Sa2	3%	3:97:205	Sa5	11%	11:89:205
Sa3	7%	7:93:205	Sa6	15%	15:85:205

In the present study, $NbSe_2$ and its derivatives, Ti-doped $NbSe_2$, were prepared by direct reaction of elements, the detailed contents are shown in Table 1. As a typical case of Sa5, the mixed powders (molar ratio: Ti:Nb:Se=11:89:205, an overdose of 10% Se) and stainless steel balls of 10mm diameter(mass ratio: mixed powders: steel balls=1:10) were sealed in a ball milling tank, which was vacuumized and filled with argon as protective gas, repeated it several times in order to the oxygen was completely drained, then the mixed powders were ball-milled in Ar atmosphere with a QM-3SP2 apparatus at 300 rpm for 24h. Subsequently, the grinded powders were put in an evacuated quartz ampoules ($\Phi8\times100$mm) as initial materials. The ampoules were heated to

maximum temperature of 700°C and 800°C by a rate of 10°C /min inside a tube furnace and the temperature was maintained at 700°C and 800°C for 1h respectively. After the completion of heating procedure, the quartz ampoules were rapidly cooled to room temperature and the as-prepared powders were obtained. The products were directly characterized without further processing by various analytic techniques. Summary of the samples doped with different amounts of Ti powders are shown in table 1.

2.2 Characterization methods

The X-ray diffraction patterns of as-prepared powders were recorded using a D8 advance (Bruker-AXS) diffractometer with Cu Ka radiation (λ = 0.1546 nm). The structure and morphology of the samples were characterized by scanning electron microscopy (SEM, JEOL JXA-840A). All the measurements were carried out at room temperature.

The as-prepared samples (Sa1−Sa6) were dispersed in paraffin base oil by the percentage of 2 wt.% via 2h ultrasonication without any active reagent, and then a series of suspended oil samples were obtained. Friction tests were performed using a UMT-2 ball-on-disc tribometer (CETR, USA) under lubricated conditions. The testing of friction reduction and wear resistance was conducted at rotating speed of 50–500 rpm and the load of 5–50N for 8–30 min. The material of the upper sample is a 40Cr stainless steel ball with a diameter of 10 mm, hardness of 62 HRC and the counterpart is a 45 steel disc of Φ40 mm×3 mm in size. The friction coefficient is automatically recorded during the contact friction.

Table 2 Latice parameters for undoped and Ti-doped $NbSe_2$ crystals.

Sample	Ti-containing	Latice parameter (a=b)	Lattice parameter (c)	Crystallite sizes/(002) plane
Sa1	0	3.44458	12.54578	87.7nm
Sa2	3%	3.41614	12.47301	38.1nm
Sa3	7%	3.40123	12.42774	31.7nm
Sa4	9%	3.39690	12.38803	21.3nm
Sa5	11%	3.44451	12.55278	27.9nm
Sa6	15%	3.44456	12.57781	>100nm

3. Results and discussion

3.1 XRD analysis

The XRD patterns for pure $NbSe_2$ and Ti-doped $NbSe_2$ are showed in figure 1, All labeled diffraction peaks in Fig.1 can be indexed to those of the pure hexagonal phase of $NbSe_2$ with calculated lattice constants of a = 3.445 Å and c = 12.55 Å, which is consistent with the values of standard card (PDF No. 65-7464). The X-ray diffractogram of $Nb_{1-x}Ti_xSe_2$ in figure 1 clearly

shows that (101) reflection becomes weaker and (002) reflection becomes stronger with the increase of Ti content, which indicates the presence of a well-stack layered structure[11-12]. The intensity of the diffraction peaks exhibited obvious widen with the introduction of Ti due to the smaller and thinner crystallite sizes (Table 2), which can confirmed that the following SEM observation. In addition, there was a very small additional reflection line related to $TiSe_2$, indicating that a small amount yield of $TiSe_2$.

The diffractogram of Nb1-xTixSe2 nanobelts is similar to that of hexagonal NbSe2, indicating that Nb1-xTixSe2 nanocrystals have been well fabricated. As the proportion of titanium addition in a certain range of 1 at.%−9 at.%, the lattice parameters become smaller due to the fact that Nb atom is replaced by Ti atom(Table 2) However, when the concentration of dopant Ti increase more than 9 at.%, the lattice parameter ‘a’ remains constant while there is a slight amount of increase in parameter ‘c’ indicates that Ti atom is embedded into interlayer position[21].

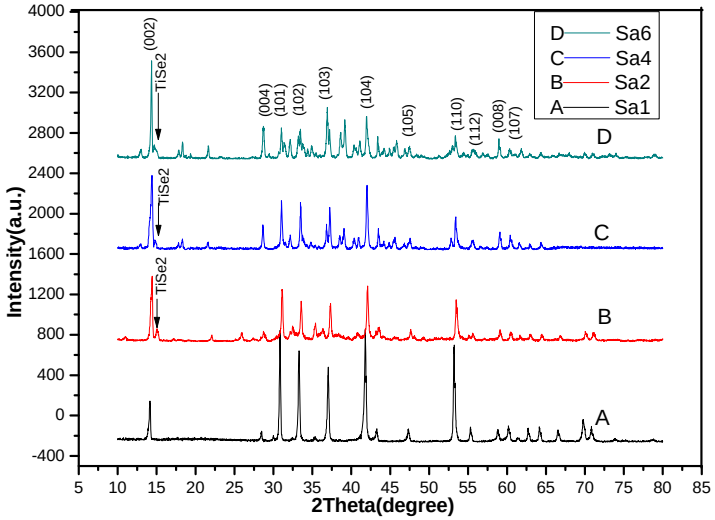

Fig. 1 XRD patterns of Undoped and Ti-doped NbSe2 nanobelts calcined at 700°C

3.2 SEM observations

The morphologies of the NbSe2 and Ti-doped NbSe2 products are primarily investigated by SEM measurement. Figure 2a shows the presence of thin, long belts-like pure $NbSe_2$ nanobelts, the average length going up to a few microns and average width about 800nm with reaction temperature of 700°C. To investigate the influence of titanium concentration on the morphology of the final products, the samples obtained at different Ti contents were analyzed. Figure 2b−2f show the SEM images of the Ti-doped $NbSe_2$ nanobelts/nanowires at the same reaction temperature. It can be clearly seen that the size of the nanobelts is decreased with the proportion of titanium addition increased in a certain limit (1 at.%−9 at.%). When introduced 9 at.% Ti powders (Fig.2d), the size reduction of the nanobelts is very significant and many nanobelts have converted to nanowires with the diameter of nearly 50 nm and the average length going up to a few microns. When the titanium addition is increased more than 9 at.% (Fig.3e, 3f), the as-prepared particles are assemble together and the size is increased.

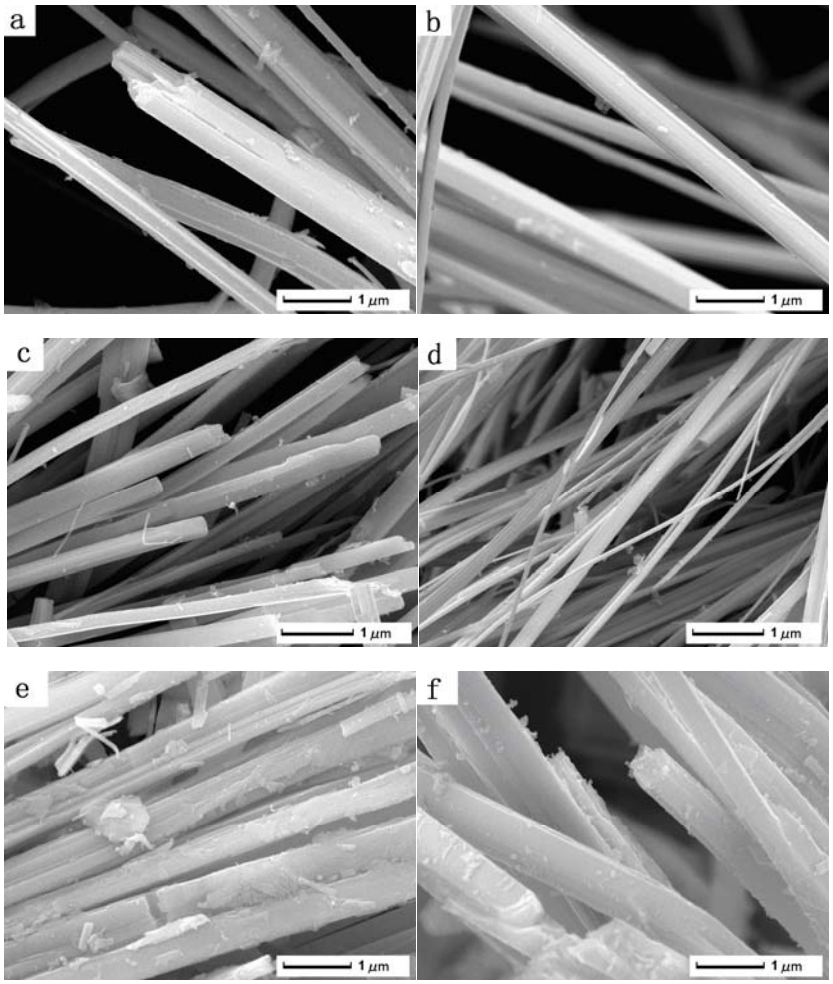

Fig.2 SEM image of the products obtained at 700°C for a-f (0, 3, 7, 9, 11, 15 at.%) Ti-doped $NbSe_2$.

The morphology of the Nb1-xTixSe2 samples obtained with the reaction temperature of 800°C are presented in figure 3, the SEM images of pure NbSe2 and Ti-doped NbSe2 nanoplates are given by contrast. The as-preapred Nb1-xTixSe2 products with reaction temperature of 800°C are mainly composed of a large amount of nanoplates with diameters of about 500nm-3μm and the thickness of about 30nm-500nm. The thickness of nanoplates changes with the titanium addition increasing, and reaches the minimum about 30 nm when Ti contents at 9 at.% (Fig.3d).

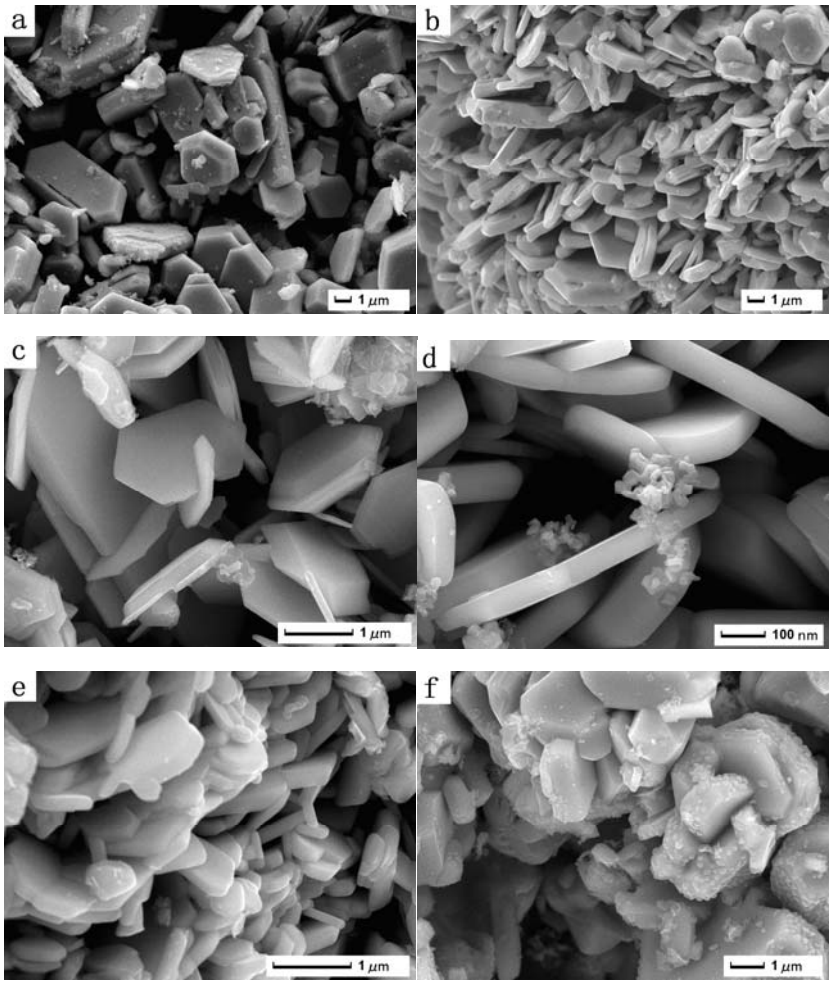

Fig.3 SEM image of the products obtained at 800°C for a-f (0, 3, 7, 9, 11, 15 at.%) Ti-doped $NbSe_2$.

From the observation made above, it is clear that the morphology of the obtained samples were affected by the reaction temperature and the contents of dopant greatly. The nanoplates with smaller size and the nanobelts with smaller width are obtained at titanium addition is 9 at. %. The conclusion is extremely in accordance with the results of XRD analysis.

3.3 Tribological properties analysis

In our previous research [17-20], $NbSe_2$ nanobelts/nanoplates exhibited excellent tribological behavior as a lubricant additive. It was found that basic oil with 2.0 wt.% NbSe2 nanobelts/nanoplates[18] indicates their excellent tribological properties. Accordingly, the tribological properties of basic oil with 2.0 wt.% Nb1-xTixSe2 nanobelts/nanoplates were investigated in this paper.

Fig. 4 depicts the comparisons of tribological properties among HVI500 basic oil without additives, the base oil containing 2 wt.% Sa1−Sa6 at the load of 35 N under the rotating speed of 400 rpm. It could easily be found from Fig. 4 that friction coefficient decreases with the addition of Nb1-xTixSe2 nanobelts, as the proportion of Ti dopant is more than 9 at.%, the friction coefficient increases. Therefore, the friction coefficient of the base oil with 2.0 wt.% Nb0.91Ti0.09Se2 nanobelts is lower and more stable than that of the base oil with other titanium concentration. The average friction coefficient of base oil with 2 wt.% Nb0.91Ti0.09Se2 nanobelts was close to 0.075, whereas it was 0.12 for the HVI500 base oil. The lubrication mechanism of layered Nb1-xTixSe2 nanobelts is associated with the shearing of the weak van der Waals bonds between the molecular layers. When Nb1-xTixSe2 nanobelts served as an additive in a base-oil, besides molecules of the base oil, Nb1-xTixSe2 nanobelts was also adsorbed on the surface of the steel friction pair to form tribofilm in the friction process. However, Fig. 4 shows that a continuous tribofilm may begin to be formed under an optimal Ti dopant concentration (9 at.%). For lower or higher Ti dopant concentrations, the formed tribofilm is incomplete.

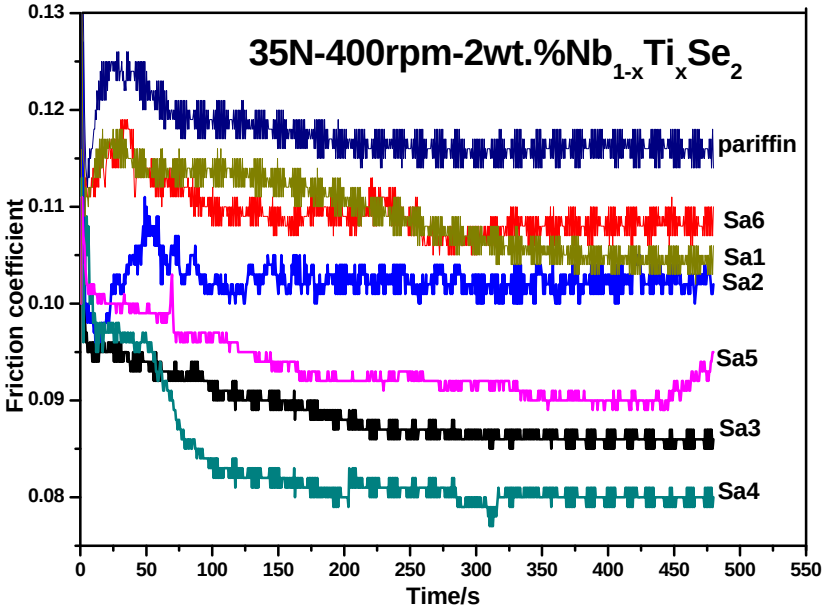

Fig. 4 *The HVI500 paraffin base oil and base oil containing 2 wt.% $Nb_{1-x}Ti_xSe_2$ nanobelts at 35N load for 480 second.*

Figure 5 represents the curve of friction of the base oil without additives, the base oil containing 2wt.% Sa1, Sa4 at the different loads (5 N, 10 N, 20 N, 30 N, 40 N) under a speed of 500 rpm for 30 min. The friction coefficient of base oil without any additives increases with the load increases. With the addition of 2.0 wt.% Nb1-xTixSe2 nanobelts/nanopaltes in base oil, the friction coefficient reduces remarkably when the load is less than 30 N. The friction coefficient of the base oil with 2.0 wt.% Nb0.91Ti0.09Se2 nanoplates is lower than that of the base oil with 2.0 wt.% Nb1-xTixSe2 nanobelts/nanoplates. Fig.6 dipects the comparisons of tribological properties among HVI500 basic oil without additives, the base oil containing 2wt.% S1, S4 at the load of 50N under diverse speeds. With the rotating speed of 100~400rpm, the friction coefficient of the base oil containing as-prepared 2wt.% (Sa1 and Sa4) nanobelts/nanoplates is always lower than that of pure base oil, and it decreases with the dopent percent of the additives is 9at.%. The reason

of this behavior may be $Nb_{0.91}Ti_{0.09}Se_2$ nanoplates with thinner and smaller size will penetrate more easily into the interface with base oil and form a continuous oil film in the concave of rubbing face, therefore, exhibit a lower friction coefficient and better anti-wear capability.

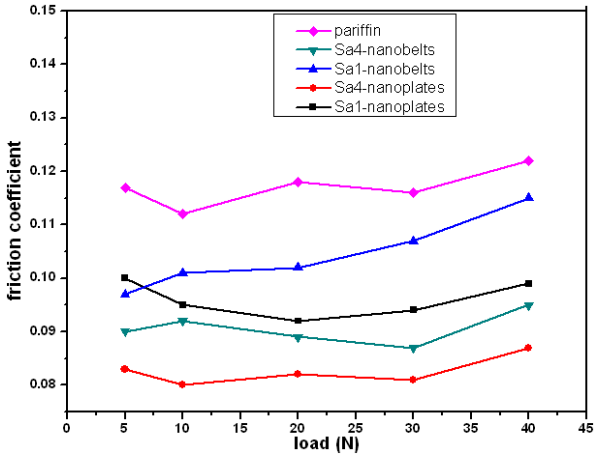

Fig. 5 Variations of friction coefficient of the paraffin base oil and the base oil containing 2 wt.% $Nb_{1-x}Ti_xSe2(x=0, 0.09)$ nanobelts/nanoplates with increasing load at 300 rpm for 30 min.

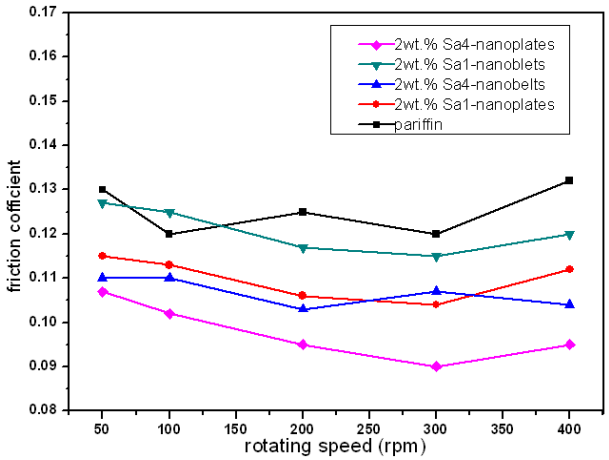

Fig.6 Frictional coefficients of HVI500 and the Basic oil with the contents of 2wt.% S1 and S4 nanobelts/nanoplates at the load of 50N under diverse speeds.

4. Conclusions

Considering all the results and discussion above, the following conclusions can be drawn.

Ti-doped NbSe2 nanobelts/nanoplates are successfully fabricated by a facile solid-state thermal reaction with micro-sized Nb and Se reacting with Ti. The morphology of $Nb_{1-x}Ti_xSe_2$ changes with reaction temperature changes, the SEM images and XRD analysis both reveal that the existence of Ti plays an important role in refining the size of $NbSe_2$ nanobelts/nanoplates.

The addition of Ti-doped NbSe2 nanobelts improved the tribological properties of base oil. The friction coefficient of the base oil with 2.0 wt.% $Nb_{0.91}Ti_{0.09}Se_2$ nanobelts presents better anti-wear capability than others.

Because of $Nb_{1-x}Ti_xSe_2$ nanoplates with thinner and smaller size will penetrate more easily into the interface with base oil, the base oil with addition of $Nb_{1-x}Ti_xSe_2$ nanoplates have lower and

more stable friction coefficient under the present experimental conditions. Furthermore, $Nb_{0.91}Ti_{0.09}Se_2$ nanoplates exibit a lower friction coefficient and better anti-wear capability than $NbSe_2$ nanobelts/nanoplates.

In a word, $Nb_{1-x}Ti_xSe_2$ particles as lubrication additive could improve tribological properties of the paraffin, and obtained the best performance when the content of Ti dopant is 9 at.%.

Acknowledgements

This work was financially supported by National Natural Science Foundation of China (51275213, 51302112), the Jiangsu National Nature Science Foundation (BK2011534,BK2011480), the Jiangsu Industry-University-Research Joint innovation Foundation (BY213065-05, BY213065-06) and Scientific and Technological Innovation Plan of Jiangsu Province in China (Grant Nos. CXLX12_0636).

References

[1] F.S. Ohuchi, T. Shimada, and B.A. Parkinson, J. Cryst. Growth. **111**, 1033 (1991).
[2] A. Kumar, and P. K. Ahluwalia, Physical B. **407**, 4627 (2012).
[3] A. Kumar, P.K. Ahluwalia, Eur. Phys. J. B. **85**, 186 (2012).
[4] A. Enyashin, S. Gemming, G. Seifert, Eur. Phys. J. (special topics) **149**, 103 (2007).
[5] C. Ataca, H. Sahin, S. Ciraci, J. Phys. Chem. C. **116**, 8983 (2012).
[6] S. Brown, J. L. Musfeldt, I.Mihut, J. B. Betts, A. Migliori, A. Zak, and R. Tenne, Nano Lett. **7**, 2365 (2007).
[7] H. Tang, C. S. Li, X. F. Yang, C. C.Mo, K. S. Cao, and F. Y. Yan, Cryst. Res. Tech. **46**, 400 (2011).
[8] G. G. Tang, H. Tang, C. S. Li, W. J. Li, and X. R. Ji, Mater. Lett. **65**, 3457 (2011).
[9] C. Feng, J. Ma, H. Li, R. Zeng, Z. Guo, and H. Liu, Mater. Res. Bull. **44**, 1811 (2009).
[10] Y.Y. Koh, Y.K. Kim, W.S. Jung, G.R. Han, et al: J. Phys. Chem. Solids. **72**, 565 (2011).
[11] X. H. Zhang, D. Zhang, H. T. Zhang, H. Tang, C. S. Li. Chalcogenide Lett. **11**, 1(2014).
[12] X. H. Zhang, H. Tang, C. S. Li, S. Chen. Chalcogenide Lett. **10**, 403(2013).
[13] D. J. Norris, A. L. Efros, and S. C. Erwin, Science. **319**, 1776 (2008).
[14] M Iavarone, G Karapetrov, J Fedor, D Rosenmann, T Nishizaki and N Kobayashi: J. Phys. Condens. Matter. **22**, 015501 (2010).
[15] Y.Y. Koh, Y.K. Kim, W.S. Jung, G.R. Han, et al: J. Phys. Chem. Solids. **72**, 565 (2011).
[16] Li C.S., Hao M.D., Liu Y.Q., Yu Y. Proc. 3rd IEEE Int. Conf. Nano/Miro Engineered and Molecular Systems, Sanya, China, 337(2008).
[17] Tang H., Cao K.S., Wu Q., ET AL., Cryst. Res. Technol. **46**, 400 (2011).
[18] J.R. Sun, G.G. Tang, C.S. Li, X.R. Ji, L. Wei, H. Tang. Micro & Nano Letters. **8**, 294(2013).
[19] S. Y. Hu, C. H. Liang, K. K. Tiong and Y. S. Huang, J. Alloy Compd. **422**, 249 (2007).
[20] S. Y. Hu, C. H. Liang, K. K. Tiong, Y . C. Lee and Y. S. Huang, J. Cryst. Growth. **285**, 408 (2005).
[21] L. Chen, C. S. Li, H. Tang, H. P. Li, X.J. Liu and J. M. RSC. Adv. **4**, 9573 (2014).